

High-energy  $\gamma$ -photon polarization in nonlinear Breit-Wheeler pair production and  $\gamma$  polarimetryFeng Wan <sup>1</sup>, Yu Wang,<sup>1</sup> Ren-Tong Guo,<sup>1</sup> Yue-Yue Chen,<sup>2</sup> Rashid Shaisultanov,<sup>3</sup> Zhong-Feng Xu,<sup>1</sup>  
Karen Z. Hatsagortsyan <sup>3,\*</sup>, Christoph H. Keitel,<sup>3</sup> and Jian-Xing Li <sup>1,†</sup><sup>1</sup>MOE Key Laboratory for Nonequilibrium Synthesis and Modulation of Condensed Matter, School of Science,  
Xi'an Jiaotong University, Xi'an 710049, China<sup>2</sup>Department of Physics, Shanghai Normal University, Shanghai 200234, China<sup>3</sup>Max-Planck-Institut für Kernphysik, Saupfercheckweg 1, 69117 Heidelberg, Germany

(Received 24 February 2020; accepted 12 August 2020; published 27 August 2020)

The interaction of an unpolarized electron beam with a counterpropagating ultraintense linearly polarized laser pulse is investigated in the quantum radiation-dominated regime. We employ a semiclassical Monte Carlo method to describe spin-resolved electron dynamics, photon emissions and polarization, and pair production. Abundant high-energy linearly polarized  $\gamma$  photons are generated intermediately during this interaction via nonlinear Compton scattering, with an average polarization degree of more than 50%, further interacting with the laser fields to produce electron-positron pairs due to the nonlinear Breit-Wheeler process. The photon polarization is shown to significantly affect the pair yield by a factor of more than 10%. The considered signature of the photon polarization in the pair's yield can be experimentally identified in a prospective two-stage setup. Moreover, with currently achievable laser facilities the signature can serve also for the polarimetry of high-energy high-flux  $\gamma$  photons.

DOI: [10.1103/PhysRevResearch.2.032049](https://doi.org/10.1103/PhysRevResearch.2.032049)

Rapid advancement of strong laser techniques [1–4] enables experimental investigation of quantum electrodynamics (QED) processes during laser-plasma and laser-electron beam interactions. Nowadays, ultrashort ultrastrong laser pulses can achieve peak intensities of about  $10^{22}$  W/cm<sup>2</sup>, with a duration of about tens of femtoseconds and an energy fluctuation  $\approx 0.01$  [5–7]. In such laser fields, QED processes become nonlinear, involving multiphoton processes [8]: A  $\gamma$  photon can be generated via nonlinear Compton scattering [9–11], or similarly a  $\gamma$  photon can create an electron-positron pair in the interaction with a strong laser wave in the nonlinear Breit-Wheeler (BW) process [12]. These processes have been experimentally observed in Refs. [13–15] and recently were considered in all-optical experimental setups [16–20]. Presently, there are many theoretical proposals aiming at  $\gamma$ -ray and pair production with ultrastrong laser fields of achievable or almost achievable intensities [21–28] and even avalanche-like electromagnetic cascades in future extreme laser intensities  $\geq 10^{24}$  W/cm<sup>2</sup> [29–36].

Recently, it has been realized that the radiation reaction due to  $\gamma$  photon emissions in laser fields can be harnessed to substantially polarize electrons [37–43] or to create polarized positrons [44,45], while it has been known for a long time

that an electron beam cannot be significantly polarized by a monochromatic laser wave [46–48]. Polarization properties of electrons, positrons, and  $\gamma$  photons in ultrastrong laser-electron beam interaction have been investigated comprehensively in Refs. [41,44,49]. It is known that an efficient way of the polarization transfer from electrons to high-energy photons can be realized via linear Compton scattering; see, e.g., Refs. [50,51]. The extension of this technique into nonlinear regime is possible [47,52–54]. In the extreme nonlinear regime, it will allow us to obtain circularly polarized brilliant  $\gamma$  rays via nonlinear Compton scattering from longitudinally spin-polarized electrons [49], highly sought in detecting schemes of vacuum birefringence in ultrastrong laser fields [55–57].

Significant efforts have been devoted to the investigation of pair production channels in ultrastrong laser-electron beam interaction [21,22,24–32]. General theory for the pair production by polarized photons in a monochromatic plane wave is given in Ref. [58]. A particular case of the multiphoton BW process with linearly polarized (LP)  $\gamma$  photons of MeV energy and moderately strong x-ray laser field is considered in Ref. [59]. The role of the  $\gamma$ -photon polarization within the BW process in a constant crossed field is considered in Ref. [60], applying a spin-averaged treatment for the photon emission by an electron. While the latter gives a hint about the photon polarization effect, it is not straightforwardly extendible to the realistic setups with tightly focused laser beams. Most simple expressions for probabilities of the polarization effects in pair production process have been obtained in local constant field approximation (LCFA) [61,62]. They show that the pair production probability depends strongly on the photon polarization and that photons emitted via nonlinear

\*k.hatsagortsyan@mpi-hd.mpg.de

†jianxing@xjtu.edu.cn

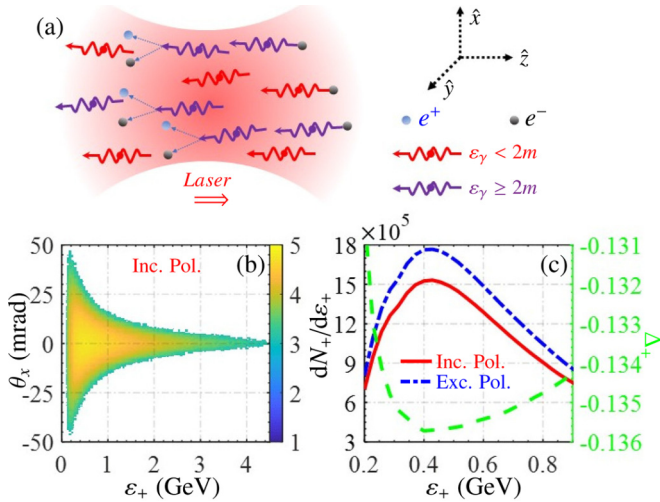


FIG. 1. (a) Scenario of nonlinear BW pair production. A LP laser pulse, polarized in the  $x$  direction and propagating along the  $+z$  direction, collides head on with an electron beam, generating LP  $\gamma$  photons, and further these pairs “ $e^+$ ” and “ $e^-$ ” indicate positron and electron, respectively. (b) Angle-resolved positron density  $\log_{10}(d^2N_+/d\epsilon_+d\theta_x)$  ( $\text{GeV}^{-1} \text{mrad}^{-1}$ ) vs the deflection angle  $\theta_x = p_x/p_z$  and the positron energy  $\epsilon_+$ , with accounting for the photon polarization. (c) Positron density  $dN_+/d\epsilon_+$  vs  $\epsilon_+$  in the cases of including (red solid) and excluding (blue dash-dotted) the photon polarization. The green dashed curve shows the relative deviation  $\Delta_+ = [(dN_+/d\epsilon_+)_{\text{Inc.Pol.}} - (dN_+/d\epsilon_+)_{\text{Exc.Pol.}}]/(dN_+/d\epsilon_+)_{\text{Exc.Pol.}}$ . The laser and electron beam parameters are given in the text [in the paragraph beginning below Eq. (1)].

Compton scattering are, in general, polarized (the LCFA probabilities have been successfully tested in experiments of pair production in channeling process, where the strong fields are produced within crystal plane and axes [63–65]). From the latter, one may expect that during the ultrastrong laser-plasma interaction the polarization of intermediate particles will strongly influence the pair production process. Therefore, we underline that for the quantitative correct predictions of pair production yields in laser-plasma interaction, the polarization-resolved treatment of intermediate particles is necessary.

In this Rapid Communication, the BW pair production process in a realistic laser-electron beam interaction setup is investigated in the quantum radiation-dominated regime. An unpolarized ultrarelativistic electron beam is considered to head-on collide with an ultrastrong LP tightly focused laser pulse, which results in radiation of highly LP high-energy  $\gamma$  photons via nonlinear Compton scattering. Further, generated polarized  $\gamma$  photons interact with the laser fields creating electron-positron pairs within the nonlinear BW process; see the interaction scenario in Fig. 1(a). We apply a fully-polarization-resolved Monte Carlo simulation method developed in Refs. [41,49] to describe the spin-resolved electron dynamics, polarized photon emissions, and pair production by the latter (see also Ref. [66] for linear and weakly nonlinear regimes). We elucidate the substantial role of intermediate polarization of photons on the pair’s yield and show how the photon polarization signature can be detected in a two-stage

setup, using laser fields of different linear polarizations and different intensities in these stages. Moreover, our results suggest an interesting application in high-resolution polarimetry of high-energy and high-flux LP  $\gamma$  rays through the pair yield.

Note that the high-resolution polarimetry of high-energy  $\gamma$  rays is an important problem in astrophysics and high-energy physics, which can be employed, e.g., to determine the nature of the emission mechanisms responsible for blazars,  $\gamma$ -ray bursts (GRBs), pulsars, and magnetars and to address problems in fundamental physics [67–70]. Current polarimetries for high-energy  $\gamma$  photons mainly employ the principles of Compton scattering and Bethe-Heitler pair production by the Coulomb fields of atoms, with an accuracy of about several percents [69,70]. The former is not efficient at photon energies larger than 100 MeV because of the kinematic suppression of the Compton rate at large scattering angles; in the latter the photon flux and polarimetry angular resolution are restricted by the converter material (damage threshold and multiple scattering), because, in particular, multiple scattering in a converter material decreases significantly the angular resolution of polarimetry [68–72]. Our polarimetry concept via nonlinear BW pair production working in a small duty cycle (determined by the laser pulse) is specifically designed for high-flux GeV  $\gamma$  photons and provides a competitive resolution.

We consider the quantum radiation-dominated regime, which requires a large nonlinear QED parameter  $\chi_e \equiv |e|\sqrt{-(F_{\mu\nu}p^\nu)^2}/m^3 \gtrsim 1$  (for electrons and positrons) [8] and  $R \equiv \alpha a_0 \chi_e \gtrsim 1$  [73]. Significant BW pair production requires the nonlinear QED parameter  $\chi_\gamma \equiv |e|\sqrt{-(F_{\mu\nu}k_\nu)^2}/m^3 \gtrsim 1$  (for  $\gamma$  photons) [8,74]. Here,  $E_0$  and  $\omega_0$  are the laser field amplitude and frequency, respectively,  $p$  and  $k_\nu$  are the 4-momenta of electron (positron) and photon, respectively,  $e$  and  $m$  are the electron charge and mass, respectively,  $F_{\mu\nu}$  is the field tensor,  $\alpha$  is the fine structure constant, and  $a_0 = |e|E_0/m\omega$  is the invariant laser field parameter. Relativistic units with  $c = \hbar = 1$  are used throughout.

In our Monte Carlo method, we treat spin-resolved electron dynamics semiclassically and photon emission and pair production quantum mechanically in LCFA [8,74–76], valid at  $a_0 \gg 1$  (for the emitted photon energies in the region  $k_- \gg \chi_e/a_0^3 p_-$ , with  $k_- = \omega - k_z$  and  $p_- = \epsilon - p_z$  being the photon and electron light-cone energies, respectively [77]). At each simulation step, the photon emission is calculated following the common algorithms [78–80] and the photon polarization following the Monte Carlo algorithm [49]. The photon Stokes parameters ( $\xi_1, \xi_2, \xi_3$ ) are defined with respect to the axes  $\hat{\mathbf{e}}_1 = \hat{\mathbf{a}} - \hat{\mathbf{v}}(\hat{\mathbf{v}}\hat{\mathbf{a}})$  and  $\hat{\mathbf{e}}_2 = \hat{\mathbf{v}} \times \hat{\mathbf{a}}$  [81], with the photon emission direction  $\hat{\mathbf{n}}$  along the ultrarelativistic electron velocity  $\mathbf{v}$ ,  $\hat{\mathbf{v}} = \mathbf{v}/|\mathbf{v}|$ , and the unit vector  $\hat{\mathbf{a}} = \mathbf{a}/|\mathbf{a}|$  along the electron acceleration  $\mathbf{a}$ . After the photon emission, the electron spin state is determined by the spin-resolved emission probabilities [41]. Between photon emissions, the spin precession is governed by the Thomas-Bargmann-Michel-Telegdi equation [82–84]. The electron spin dynamics simulated by our method is in accordance with the results of the CAIN code [66], applicable for simulating the electron-laser as well as beam-beam collisions. Note that the latter use a slightly different Monte Carlo algorithm for spin evolution (the spin

quantization axis after the photon emission is chosen along the average spin direction, with further quantum mechanical spin rotation due to the probability of no photon emissions).

We describe the polarized photon conversion to electron-positron pair by the probabilities of the pair production. The latter, summing over the pair spins, is derived in the leading-order contribution with respect to  $1/\gamma_e$  via the QED operator method of Baier-Katkov [62]:

$$\frac{d^2 W_{\text{pair}}}{d\varepsilon_+ dt} = \frac{\alpha m^2}{\sqrt{3\pi} \varepsilon_\gamma^2} \left\{ \text{Int} K_{\frac{1}{3}}(\rho) + \left( \frac{\varepsilon_+^2 + \varepsilon_-^2}{\varepsilon_+ \varepsilon_-} - \xi_3 \right) K_{\frac{2}{3}}(\rho) \right\}, \quad (1)$$

where  $\varepsilon_-$  and  $\varepsilon_+$  are the energies of created electron and positron, respectively, with the photon energy  $\varepsilon_\gamma = \varepsilon_- + \varepsilon_+$ ,  $\rho \equiv 2\varepsilon_\gamma^2 / (3\chi_\gamma \varepsilon_+ \varepsilon_-)$ ,  $\text{Int} K_{\frac{1}{3}}(\rho) \equiv \int_\rho^\infty dx K_{\frac{1}{3}}(x)$ , and  $K_n$  is the  $n$ -order modified Bessel function of the second kind. In this relativistic setup, the emitted  $\gamma$  photon is assumed to propagate along the radiating electron momentum, and the pair is assumed to do so along the parent  $\gamma$ -photon momentum. Note that by averaging over the photon polarization one obtains the known pair production probability  $W_{\text{pair}}^{\text{Exc.Pol.}}$  [74] and  $W_{\text{pair}} = W_{\text{pair}}^{\text{Exc.Pol.}} - \xi_3 W_\xi$ . When including polarization in Eq. (1), the Stokes parameters are transformed from the photon emission frame ( $\hat{\mathbf{e}}_1, \hat{\mathbf{e}}_2, \hat{\mathbf{n}}$ ) to the pair production frame ( $\hat{\mathbf{e}}'_1, \hat{\mathbf{e}}'_2, \hat{\mathbf{n}}$ ), where  $\hat{\mathbf{e}}'_1 = [\mathbf{E} - \hat{\mathbf{n}} \cdot (\hat{\mathbf{n}} \cdot \mathbf{E}) + \hat{\mathbf{n}} \times \mathbf{B}] / |\mathbf{E} - \hat{\mathbf{n}} \cdot (\hat{\mathbf{n}} \cdot \mathbf{E}) + \hat{\mathbf{n}} \times \mathbf{B}|$  and  $\hat{\mathbf{e}}'_2 = \hat{\mathbf{n}} \times \hat{\mathbf{e}}'_1$ , with the electric and magnetic field components  $\mathbf{E}$  and  $\mathbf{B}$ ; see Ref. [85].

The impact of the photon polarization on the BW pair production is quantitatively demonstrated in Figs. 1(b) and 1(c). The employed laser and electron beam parameters are the following. A realistic tightly focused Gaussian LP laser pulse [85,86] propagates along  $+z$  direction (polar angle  $\theta_l = 0^\circ$ ), with peak intensity  $I_0 \approx 3.45 \times 10^{21}$  W/cm<sup>2</sup> ( $a_0 = 50$ ), wavelength  $\lambda_0 = 1$   $\mu\text{m}$ , pulse duration  $\tau = 15T_0$  with period  $T_0$ , and focal radius  $w_0 = 5$   $\mu\text{m}$ . A cylindrical unpolarized electron beam propagates along the  $-z$  direction (polar angle  $\theta_e = 180^\circ$ ), with initial kinetic energy  $\varepsilon_0 = 10$  GeV, angular divergence  $\Delta\theta = 0.3$  mrad, energy spread  $\Delta\varepsilon_0/\varepsilon_0 = 0.06$ , beam radius  $w_e = \lambda_0$ , beam length  $L_e = 5\lambda_0$ , emittance  $\varepsilon_e \approx 3 \times 10^{-4}$  mm mrad, electron number  $N_e = 5 \times 10^6$ , and density  $n_e \approx 3.18 \times 10^{17}$  cm<sup>-3</sup> with a transversely Gaussian and longitudinally uniform distribution. The electron beam parameters are typical for laser-plasma acceleration [87]. The pair production and radiation reaction are significant at these parameters as  $\chi_e \approx 2.47$ ,  $\text{Max}(\chi_\gamma) \approx 2.34$ , and  $R \approx 1$ , while avalanche-like cascades are suppressed.

Our simulations show that radiated  $\gamma$  photons are dominantly LP with an average polarization of  $\bar{\xi}_3 \approx 55.64\%$ . The further produced pairs are characterized in Fig. 1(b). The transverse angular spread of the positrons is about 90 mrad, and the energies are mainly in the region of  $0.2$  GeV  $\lesssim \varepsilon_+ \lesssim 4.4$  GeV. Integrating over the angular distribution, we show the energy distribution of positrons in Fig. 1(c). When the intermediate photon polarization is accounted for, the pair (positron) yield decreases. The relative difference reaches the maximum of  $|\Delta_+| \approx 13.6\%$  at  $\varepsilon_+ \approx 0.4$  GeV, and the average relative deviation  $\bar{\Delta}_+ = (N_+^{\text{Inc.Pol.}} - N_+^{\text{Exc.Pol.}}) / N_+^{\text{Exc.Pol.}} \approx -13.44\%$ . For the given parameters, the positron

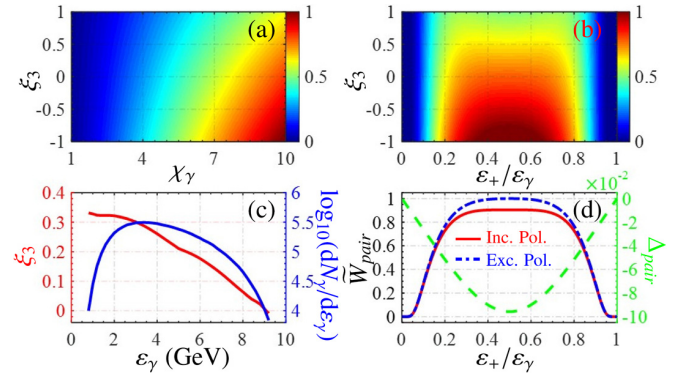


FIG. 2. (a) Normalized pair production probability  $\tilde{W}_{\text{pair}}$ , integrating over  $\varepsilon_+$  and scaled by its maximal value at  $(\chi_\gamma, \xi_3) = (10, -1)$  in the demonstrated parametric region, vs  $\chi_\gamma$  and  $\xi_3$ . (b)  $\tilde{W}_{\text{pair}}$  with  $\chi_\gamma = 2.34$  (corresponding to  $\bar{\chi}_\gamma$  of Fig. 1), scaled by its maximal value at  $(\varepsilon_+/\varepsilon_\gamma, \xi_3) = (0.5, -1)$  in the demonstrated parametric region, vs  $\varepsilon_+/\varepsilon_\gamma$  and  $\xi_3$ . (c)  $\xi_3$  (red) and density  $\log_{10}(dN_\gamma/d\varepsilon_\gamma)$  (blue) of emitted  $\gamma$  photons, which eventually split to pairs, vs  $\varepsilon_\gamma$ . (d)  $\tilde{W}_{\text{pair}}$  vs  $\varepsilon_+/\varepsilon_\gamma$  for the cases of including polarization with  $\xi_3 = 25.91\%$  (red solid) and excluding polarization (i.e.,  $\xi_3 = 0$ , blue dash-dotted), respectively. The green dashed curve indicates the relative deviation of the pair creation probabilities  $\Delta_{\text{pair}} = (\tilde{W}_{\text{pair}}^{\text{Inc.Pol.}} - \tilde{W}_{\text{pair}}^{\text{Exc.Pol.}}) / \tilde{W}_{\text{pair}}^{\text{Exc.Pol.}}$ . Other laser and electron beam parameters are the same as those in Fig. 1.

number is  $N_+^{\text{Inc.Pol.}} \approx 1.36 \times 10^6 \approx N_e \times 27.2\%$ , and thus, the deviation of about 13.44% is remarkable but cannot be directly measured in an experiment. We propose the experimental observation of the discussed effect in a two-stage setup discussed below.

The physical reason for the intermediate polarization effect is analyzed in Fig. 2. According to Eq. (1),  $W_{\text{pair}}$  depends on the parameters  $\xi_3$ ,  $\chi_\gamma$ , and  $\varepsilon_+/\varepsilon_\gamma$ . As illustrated in Figs. 2(a) and 2(b),  $W_{\text{pair}}$  continuously decreases (increases) with the increase of  $\xi_3$  ( $\chi_\gamma$ ), and has a symmetric distribution with respect to  $\varepsilon_+/\varepsilon_\gamma$ . Intermediate  $\gamma$  photons, which are radiated by the electrons and eventually split to pairs, are LP with an average polarization  $\bar{\xi}_3 \approx 25.91\%$  (lower than that of all emitted  $\gamma$  photons), as demonstrated in Fig. 2(c), and the corresponding pair production probability is smaller than that excluding polarization, in particular, in the region of  $0.2 \lesssim \varepsilon_+/\varepsilon_\gamma \lesssim 0.8$  in Fig. 2(d). Consequently, the pair yield of consistently including the photon polarization is much smaller than that with averaging over the polarization, as shown in Fig. 1(c).

This photon polarization effect is robust with respect to the laser and electron beam parameters. As the laser field parameter  $a_0$  varies from 40 to 60, the laser pulse duration from 12 to 18 cycles, and the initial kinetic energy of the electron beam  $\varepsilon_0$  from 8 to 10 GeV, the pair production parameter  $\tilde{\Delta}_+$  changes less than 10% [85]. It stays almost identical for the cases of larger angular divergence of  $\Delta\theta = 1$  mrad, larger energy spread  $\Delta\varepsilon_0/\varepsilon_0 = 0.1$ , and different colliding angle  $\theta_e = 175^\circ$  [85]. In the case of employing a circularly polarized laser pulse, the average polarization of emitted  $\gamma$  photons by the unpolarized electron beam is rather small, and consequently, the considered effect cannot be identified [85].

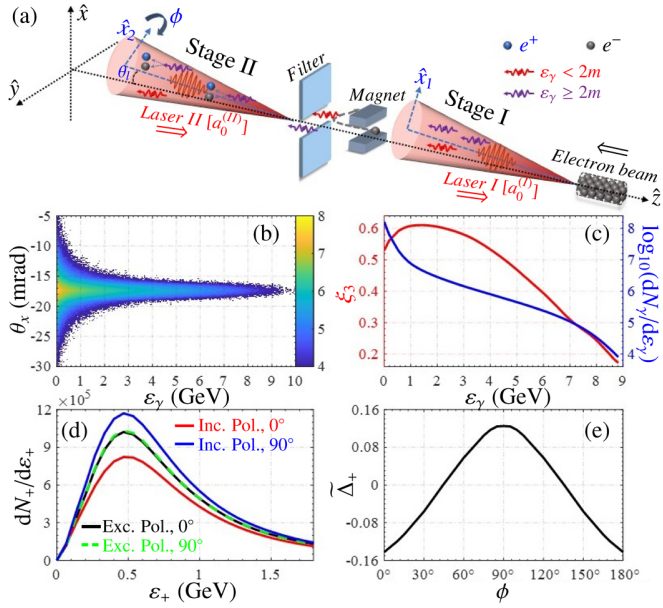


FIG. 3. (a) Two-stage scenario for detection of the considered effect of the photon polarization. In stages I and II, the laser fields have different LP along  $\hat{x}_1$  and  $\hat{x}_2$ , and different intensities,  $a_0^{(I)} = 20$  ( $\text{Max}(\chi_\gamma) \approx 0.91$ ) and  $a_0^{(II)} = 50$ , respectively;  $\phi$  is the rotation angle of the polarization  $\hat{x}_2$  with respect to  $\hat{x}_1$ . (b)  $\log_{10}(d^2N_\gamma/d\epsilon_\gamma d\theta_x)$  vs  $\theta_x$  and  $\epsilon_\gamma$ , generated in stage I. (c)  $\log_{10}(dN_\gamma/d\epsilon_\gamma)$  (blue), calculated by integrating  $d^2N_\gamma/d\epsilon_\gamma d\theta_x$  in panel (b) over  $\theta_x$  from  $-25$  mrad to  $-10$  mrad, and the corresponding  $\xi_3$  (red) vs  $\epsilon_\gamma$ . (d)  $dN_+/d\epsilon_+$  vs  $\epsilon_+$ , produced in stage II, in the cases of including polarization with  $\phi = 0^\circ$  (red solid,  $\hat{x}_2 \parallel \hat{x}_1$ ) and  $90^\circ$  (blue solid,  $\hat{x}_2 \perp \hat{x}_1$ ) and excluding polarization with  $\phi = 0^\circ$  (black solid) and  $90^\circ$  (green dashed), respectively; (e)  $\tilde{\Delta}_+$  vs  $\phi$ . Other laser and electron beam parameters are the same as those in Fig. 1.

Experimental verification of the intermediate photon polarization can be carried out in a all-optical two-stage setup, which is similar to those generally used to probe vacuum birefringence [55,56], and a similar setup has been realized with crystals [63–65]. In both stages of our setup, LP laser pulses are used, but with different polarization directions. In stage I, a relatively low laser intensity  $a_0^{(I)} = 20$  [ $\text{Max}(\chi_\gamma) \approx 0.91$ ] is used for  $\gamma$ -photon production via nonlinear Compton scattering [see Fig. 3(b)], which can produce much higher flux  $\gamma$  rays than the linear Compton scattering and suppress the pair creation, while in stage II a higher laser intensity  $a_0^{(II)} = 50$  is used for pair production via the nonlinear BW process. When the laser polarization direction in stage II is parallel to that in stage I ( $\phi = 0^\circ$ ,  $\hat{x}_2 \parallel \hat{x}_1$ ), the pair yield of including polarization is much smaller than that excluding polarization,  $N_+^{\text{Inc.Pol.}} < N_+^{\text{Exc.Pol.}}$ , with  $\tilde{\Delta}_+ \approx -14.23\%$  [see Fig. 3(d)] because  $\xi_3$  in this frame is positive with  $\bar{\xi}_3 \approx 55.54\%$  [see Fig. 3(c)]. When the polarization direction in stage II is rotated by  $\phi = 90^\circ$ ,  $\xi_3$  of  $\gamma$  photons in the rotated frame becomes negative,  $\bar{\xi}_3 \approx -55.54\%$ . Consequently, we have  $N_+^{\text{Inc.Pol.}} > N_+^{\text{Exc.Pol.}}$ , with  $\tilde{\Delta}_+ \approx 12.52\%$  [see Fig. 3(d)]. It is clear that in the case of neglecting the photon polarization, the rotation of the laser polarization in stage II would not affect the pair yield. We can explain also why the absolute value  $|\tilde{\Delta}_+|$  in the case of  $\phi = 0^\circ$  is slightly larger than that

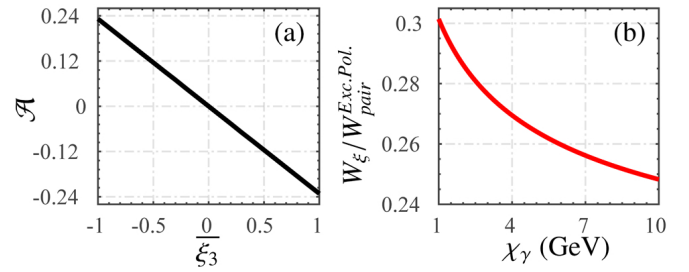


FIG. 4. Polarimetry for high-flux high-energy  $\gamma$  photons. (a) The asymmetry parameter  $\mathcal{A}$ , defined in the text, vs  $\xi_3$ . (b)  $W_\xi/W_{\text{pair}}^{\text{Exc.Pol.}}$  vs  $\chi_\gamma$  by summing over  $\epsilon_+/\epsilon_\gamma$ . The average energy of  $\gamma$  photons  $\bar{\epsilon}_\gamma = 4.32$  GeV (corresponding to  $\bar{\epsilon}_\gamma$  in Fig. 1), with an angular divergence  $\Delta\theta_\gamma = 0.3$  mrad and an energy spread  $\Delta\epsilon_\gamma/\epsilon_\gamma = 6\%$ . The scattering laser parameters are the same as those in Fig. 1.

of  $\phi = 90^\circ$ . The reason is that the pair production probability is  $W_{\text{pair}} = W_{\text{pair}}^{\text{Exc.Pol.}} - \xi_3 W_\xi$  in a single formation length, but within  $n$  formation lengths it is  $W_n = 1 - (1 - W_{\text{pair}})^n = 1 - [1 - (W_{\text{pair}}^{\text{Exc.Pol.}} - \xi_3 W_\xi)]^n$ , which is asymmetric with respect to  $\xi_3$ . Thus, the dependence of  $\tilde{\Delta}_+$  on the rotation angle  $\phi$  demonstrated in Fig. 3(e) can be a measurable experimental signature of the considered photon polarization effect.

Finally, we investigate to which extent the nonlinear Breit-Wheeler process can be used for polarimetry for high-flux multi-GeV  $\gamma$  photons. A  $\gamma$  photon beam collides head on with an ultrastrong LP laser pulse, and the interaction scenario is similar to stage II in Fig. 3(a). The procedure of determining the LP Stokes parameters  $\bar{\xi}_1$  and  $\bar{\xi}_3$  of the given photon beam is the following. For the  $\bar{\xi}_3$  determination, the laser polarization first is fixed along the  $x$  direction, and the positron (pair) yield  $N_+|_{\phi=0^\circ}$  is measured. Then, the laser polarization is rotated by  $90^\circ$ , and again  $N_+|_{\phi=90^\circ}$  is measured, which is different from  $N_+|_{\phi=0^\circ}$  since  $\bar{\xi}_3$  changes with the rotation of the laser polarization; see similar interpretation in Fig. 3. Thus,  $\bar{\xi}_3$  can be deduced by an asymmetry parameter

$$\mathcal{A} = \frac{N_+|_{\phi=0^\circ} - N_+|_{\phi=90^\circ}}{N_+|_{\phi=0^\circ} + N_+|_{\phi=90^\circ}}, \quad (2)$$

and the relation of  $\mathcal{A}$  to  $\bar{\xi}_3$  is shown in Fig. 4(a). In the same way, the Stokes parameter  $\bar{\xi}_1$  can be determined via another asymmetry parameter  $\mathcal{A}'$ , first fixing the laser polarization along the axis of  $\phi = 45^\circ$  and then rotating by  $90^\circ$  ( $\phi = 135^\circ$ ).

The resolution of the polarization measurement can be estimated via the statistical uncertainty  $\delta\mathcal{A}/\Delta\mathcal{A} = 1/(\Delta\mathcal{A}\sqrt{N_+})$  [88], where the total number of pairs  $N_+ = \mathcal{R}_{\text{pair}}N_\gamma$  is determined by the pair production rate  $\mathcal{R}_{\text{pair}} \approx 37.98\%$  and  $\Delta\mathcal{A} = \text{Max}(\mathcal{A}) - \text{Min}(\mathcal{A}) \approx 0.4634$ , calculated with the given parameters. For instance, in the case of the laser-driven polarized  $\gamma$  rays [49], we have  $N_\gamma \approx 10^6$ , and the resolution is about 0.35%. As the photon flux increases, the resolution increases accordingly. The resolution improves as well with the increase of the pair yield, which takes place when increasing  $\chi_\gamma$  (see analysis in Fig. 2), and with the increase of the asymmetry parameter  $\Delta\mathcal{A} \sim W_\xi/W_{\text{pair}}^{\text{Exc.Pol.}}$ . The latter, however, decreases with larger  $\chi_\gamma$  [see Fig. 4(b)]. Because of the opposite behaviors of  $N_+$  and  $\Delta\mathcal{A}$  with the

variation of  $\chi_\gamma \propto a_0 \varepsilon_\gamma$ , the resolution is quite stable with respect to the changes of the laser intensity and the  $\gamma$ -photon energy. Moreover, the resolution does not vary much and remains well below 1% with a shorter or longer laser pulse, a larger energy spread  $\Delta\varepsilon_\gamma/\varepsilon_\gamma = 0.1$ , a larger angular divergence  $\Delta\theta_\gamma = 1$  mrad, and a different colliding angle  $\theta_\gamma = 175^\circ$  [85]. The proposed polarimetry based on the BW process avoids limitations of  $\gamma$ -ray polarimetry via the BH process [68–72] with respect to the  $\gamma$ -ray flux and angular resolution, imposed by the convertor material in the latter.

In conclusion, the impact of intermediate photon polarization on nonlinear BW pair production during LP laser-electron beam interaction is investigated in the quantum radiation-dominated regime. The photon polarization is shown to significantly affect the pair yield by a factor of more than 13%. Thus, for accurate Monte Carlo simulations of laser-electron

beam interaction it is crucial to treat the electron spin and polarization of intermediate particles, even for simulations of those processes where the polarization of the final particles is not in the center of interest. Our analysis suggests that the considered signature of the photon polarization is experimentally detectable in a two-stage all-optical setup. Moreover, we provide a polarimetry method specifically designed for high-flux high-energy  $\gamma$  rays in the GeV range, which provides competitive resolution with currently feasible laser facilities, and is likely to be useful in astrophysics and high-energy physics.

This work is supported by the National Natural Science Foundation of China (Grants No. 11874295, No. 11875219, and No. 11905169), and the National Key R&D Program of China (Grant No. 2018YFA0404801).

- 
- [1] The Extreme Light Infrastructure (ELI) [<http://www.eli-beams.eu/en/facility/lasers/>].
- [2] The Vulcan facility [<http://www.clf.stfc.ac.uk/Pages/The-Vulcan-10-Petawatt-Project.aspx>].
- [3] Exawatt Center for Extreme Light Studies (XCELS) [<http://www.xcels.iapras.ru/>].
- [4] The Center for Relativistic Laser Science (CoReLS) [[https://www.ibs.re.kr/eng/sub02\\_03\\_05.do](https://www.ibs.re.kr/eng/sub02_03_05.do)].
- [5] J. W. Yoon, C. Jeon, J. Shin, S. K. Lee, H. W. Lee, I. W. Choi, H. T. Kim, J. H. Sung, and C. H. Nam, Achieving the laser intensity of  $5.5 \times 10^{22}$  w/cm<sup>2</sup> with a wavefront-corrected multi-pw laser, *Opt. Express* **27**, 20412 (2019).
- [6] C. N. Danson, C. Haefner, J. Bromage, T. Butcher, J.-C. F. Chanteloup, E. A. Chowdhury, A. Galvanauskas, L. A. Gizzi, J. Hein, D. I. Hillier *et al.*, Petawatt and exawatt class lasers worldwide, *High Power Laser Sci. Eng.* **7**, e54 (2019).
- [7] S. Gales, K. A. Tanaka, D. L. Balabanski, F. Negoita, D. Stutman, O. Tesileanu, C. A. Ur, D. Ursescu, I. Andrei, S. Ataman, M. O. Cernaianu, L. D’Alessi, I. Dancus, B. Diaconescu, N. Djourelou, D. Filipescu, P. Ghenuche, D. G. Ghita, C. Matei, K. Seto, M. Zeng, and N. V. Zamfir, The extreme light infrastructure–nuclear physics (ELI-NP) facility: New horizons in physics with 10 PW ultra-intense lasers and 20 MeV brilliant gamma beams, *Rep. Prog. Phys.* **81**, 094301 (2018).
- [8] V. I. Ritus, Quantum effects of the interaction of elementary particles with an intense electromagnetic field, *J. Sov. Laser Res.* **6**, 497 (1985).
- [9] I. I. Goldman, Intensity effects in Compton scattering, *Sov. Phys. JETP* **19**, 954 (1964).
- [10] A. I. Nikishov and V. I. Ritus, Quantum processes in the field of a plane electromagnetic wave and in a constant field. I, *Sov. Phys. JETP* **19**, 529 (1964).
- [11] L. S. Brown and T. W. B. Kibble, Interaction of intense laser beams with electrons, *Phys. Rev.* **133**, A705 (1964).
- [12] H. R. Reiss, Absorption of light by light, *J. Math. Phys.* **3**, 59 (1962).
- [13] C. Bula, K. T. McDonald, E. J. Prebys, C. Bamber, S. Boege, T. Kotseroglou, A. C. Melissinos, D. D. Meyerhofer, W. Ragg, D. L. Burke, R. C. Field, G. Horton-Smith, A. C. Odian, J. E. Spencer, D. Walz, S. C. Berridge, W. M. Bugg, K. Shmakov, and A. W. Weidemann, Observation of Nonlinear Effects in Compton Scattering, *Phys. Rev. Lett.* **76**, 3116 (1996).
- [14] D. L. Burke, R. C. Field, G. Horton-Smith, J. E. Spencer, D. Walz, S. C. Berridge, W. M. Bugg, K. Shmakov, A. W. Weidemann, C. Bula, K. T. McDonald, E. J. Prebys, C. Bamber, S. J. Boege, T. Koffas, T. Kotseroglou, A. C. Melissinos, D. D. Meyerhofer, D. A. Reis, and W. Ragg, Positron Production in Multiphoton Light-By-Light Scattering, *Phys. Rev. Lett.* **79**, 1626 (1997).
- [15] C. Bamber, S. J. Boege, T. Koffas, T. Kotseroglou, A. C. Melissinos, D. D. Meyerhofer, D. A. Reis, W. Ragg, C. Bula, K. T. McDonald, E. J. Prebys, D. L. Burke, R. C. Field, G. Horton-Smith, J. E. Spencer, D. Walz, S. Berridge, W. M. Bugg, K. Shmakov, and A. W. Weidemann, Studies of nonlinear QED in collisions of 46.6 GeV electrons with intense laser pulses, *Phys. Rev. D* **60**, 092004 (1999).
- [16] G. Sarri, D. J. Corvan, W. Schumaker, J. M. Cole, A. Di Piazza, H. Ahmed, C. Harvey, C. H. Keitel, K. Krushelnick, S. P. D. Mangles, Z. Najmudin, D. Symes, A. G. R. Thomas, M. Yeung, Z. Zhao, and M. Zepf, Ultrahigh Brilliance Multi-mev  $\gamma$ -Ray Beams from Nonlinear Relativistic Thomson Scattering, *Phys. Rev. Lett.* **113**, 224801 (2014).
- [17] G. Sarri, K. Poder, J. M. Cole, W. Schumaker, A. Di Piazza, B. Reville, T. Dzelzainis, D. Doria, L. A. Gizzi, G. Grittani, S. Kar, C. H. Keitel, K. Krushelnick, S. Kuschel, S. P. D. Mangles, Z. Najmudin, N. Shukla, L. O. Silva, D. Symes, A. G. R. Thomas, M. Vargas, J. Vieira, and M. Zepf, Generation of neutral and high-density electron-positron pair plasmas in the laboratory, *Nat. Commun.* **6**, 6747 (2015).
- [18] W. Yan, C. Fruhling, G. Golovin, D. Haden, J. Luo, P. Zhang, B. Zhao, J. Zhang, C. Liu, M. Chen, S. Chen, S. Banerjee, and D. Umstadter, High-order multiphoton Thomson scattering, *Nat. Photon.* **11**, 514 (2017).
- [19] J. M. Cole, K. T. Behm, E. Gerstmayr, T. G. Blackburn, J. C. Wood, C. D. Baird, M. J. Duff, C. Harvey, A. Ilderton, A. S. Joglekar, K. Krushelnick, S. Kuschel, M. Marklund, P. McKenna, C. D. Murphy, K. Poder, C. P. Ridgers, G. M. Samarin, G. Sarri, D. R. Symes, A. G. R. Thomas, J. Warwick, M. Zepf, Z. Najmudin, and S. P. D. Mangles, Experimental Evidence of Radiation Reaction in the Collision of a High-Intensity

- Laser Pulse with a Laser-Wakefield Accelerated Electron Beam, *Phys. Rev. X* **8**, 011020 (2018).
- [20] K. Poder, M. Tamburini, G. Sarri, A. Di Piazza, S. Kuschel, C. D. Baird, K. Behm, S. Bohlen, J. M. Cole, D. J. Corvan, M. Duff, E. Gerstmayr, C. H. Keitel, K. Krushelnick, S. P. D. Mangles, P. McKenna, C. D. Murphy, Z. Najmudin, C. P. Ridgers, G. M. Samarin, D. R. Symes, A. G. R. Thomas, J. Warwick, and M. Zepf, Experimental Signatures of the Quantum Nature of Radiation Reaction in the Field of an Ultraintense Laser, *Phys. Rev. X* **8**, 031004 (2018).
- [21] H. Hu, C. Müller, and C. H. Keitel, Complete QED Theory of Multiphoton Trident Pair Production in Strong Laser Fields, *Phys. Rev. Lett.* **105**, 080401 (2010).
- [22] A. I. Titov, H. Takabe, B. Kämpfer, and A. Hosaka, Enhanced Subthreshold  $e^+e^-$  Production in Short Laser Pulses, *Phys. Rev. Lett.* **108**, 240406 (2012).
- [23] H. Hu and C. Müller, Relativistic Three-Body Recombination with the QED Vacuum, *Phys. Rev. Lett.* **107**, 090402 (2011).
- [24] C. P. Ridgers, C. S. Brady, R. Duclous, J. G. Kirk, K. Bennett, T. D. Arber, and A. R. Bell, Dense electron-positron plasmas and bursts of  $\gamma$ -rays from laser-generated quantum electrodynamic plasmas, *Phys. Plasmas* **20**, 056701 (2013).
- [25] V. F. Bashmakov, E. N. Nerush, I. Y. Kostyukov, A. M. Fedotov, and N. B. Narozhny, Effect of laser polarization on quantum electrodynamic cascading, *Phys. Plasmas* **21**, 013105 (2014).
- [26] T. Nakamura and T. Hayakawa, Laser-driven  $\gamma$ -ray, positron, and neutron source from ultra-intense laser-matter interactions, *Phys. Plasmas* **22**, 083113 (2015).
- [27] T. G. Blackburn, A. Ilderton, C. D. Murphy, and M. Marklund, Scaling laws for positron production in laser-electron-beam collisions, *Phys. Rev. A* **96**, 022128 (2017).
- [28] O. Olugh, Z.-L. Li, B.-S. Xie, and R. Alkofer, Pair production in differently polarized electric fields with frequency chirps, *Phys. Rev. D* **99**, 036003 (2019).
- [29] M. Marklund and P. K. Shukla, Nonlinear collective effects in photon-photon and photon-plasma interactions, *Rev. Mod. Phys.* **78**, 591 (2006).
- [30] G. A. Mourou, T. Tajima, and S. V. Bulanov, Optics in the relativistic regime, *Rev. Mod. Phys.* **78**, 309 (2006).
- [31] A. R. Bell and J. G. Kirk, Possibility of Prolific Pair Production with High-Power Lasers, *Phys. Rev. Lett.* **101**, 200403 (2008).
- [32] A. Di Piazza, C. Müller, K. Z. Hatsagortsyan, and C. H. Keitel, Extremely high-intensity laser interactions with fundamental quantum systems, *Rev. Mod. Phys.* **84**, 1177 (2012).
- [33] M. Vranic, T. Grismayer, R. A. Fonseca, and L. O. Silva, Electron-positron cascades in multiple-laser optical traps, *Plasma Phys. Controlled Fusion* **59**, 014040 (2016).
- [34] T. Grismayer, M. Vranic, J. L. Martins, R. A. Fonseca, and L. O. Silva, Laser absorption via quantum electrodynamics cascades in counter propagating laser pulses, *Phys. Plasmas* **23**, 056706 (2016).
- [35] M. Tamburini, A. Di Piazza, and C. H. Keitel, Laser-pulse-shape control of seeded qed cascades, *Sci. Rep.* **7**, 5694 (2017).
- [36] A. Gonoskov, A. Bashinov, S. Bastrakov, E. Efimenko, A. Ilderton, A. Kim, M. Marklund, I. Meyerov, A. Muraviev, and A. Sergeev, Ultrabright GeV Photon Source Via Controlled Electromagnetic Cascades in Laser-Dipole Waves, *Phys. Rev. X* **7**, 041003 (2017).
- [37] D. Del Sorbo, D. Seipt, T. G. Blackburn, A. G. R. Thomas, C. D. Murphy, J. G. Kirk, and C. P. Ridgers, Spin polarization of electrons by ultraintense lasers, *Phys. Rev. A* **96**, 043407 (2017).
- [38] D. Del Sorbo, D. Seipt, A. G. R. Thomas, and C. P. Ridgers, Electron spin polarization in realistic trajectories around the magnetic node of two counter-propagating, circularly polarized, ultra-intense lasers, *Plasma Phys. Controlled Fusion* **60**, 064003 (2018).
- [39] D. Seipt, D. Del Sorbo, C. P. Ridgers, and A. G. R. Thomas, Theory of radiative electron polarization in strong laser fields, *Phys. Rev. A* **98**, 023417 (2018).
- [40] D. Seipt, D. Del Sorbo, C. P. Ridgers, and A. G. R. Thomas, Ultrafast polarization of an electron beam in an intense bichromatic laser field, *Phys. Rev. A* **100**, 061402(R) (2019).
- [41] Y.-F. Li, R. Shaisultanov, K. Z. Hatsagortsyan, F. Wan, C. H. Keitel, and J.-X. Li, Ultrarelativistic Electron-Beam Polarization in Single-Shot Interaction with an Ultraintense Laser Pulse, *Phys. Rev. Lett.* **122**, 154801 (2019).
- [42] H.-H. Song, W.-M. Wang, J.-X. Li, Y.-F. Li, and Y.-T. Li, Spin-polarization effects of an ultrarelativistic electron beam in an ultraintense two-color laser pulse, *Phys. Rev. A* **100**, 033407 (2019).
- [43] Y.-F. Li, R.-T. Guo, R. Shaisultanov, K. Z. Hatsagortsyan, and J.-X. Li, Electron Polarimetry with Nonlinear Compton Scattering, *Phys. Rev. Appl.* **12**, 014047 (2019).
- [44] Y.-Y. Chen, P.-L. He, R. Shaisultanov, K. Z. Hatsagortsyan, and C. H. Keitel, Polarized Positron Beams Via Intense Two-Color Laser Pulses, *Phys. Rev. Lett.* **123**, 174801 (2019).
- [45] F. Wan, R. Shaisultanov, Y.-F. Li, K. Z. Hatsagortsyan, C. H. Keitel, and J.-X. Li, Ultrarelativistic polarized positron jets via collision of electron and ultraintense laser beams, *Phys. Lett. B* **800**, 135120 (2020).
- [46] G. L. Kotkin, V. G. Serbo, and V. I. Telnov, Electron (positron) beam polarization by Compton scattering on circularly polarized laser photons, *Phys. Rev. ST Accel. Beams* **6**, 011001 (2003).
- [47] D. Yu. Ivanov, G. L. Kotkin, and V. G. Serbo, Complete description of polarization effects in emission of a photon by an electron in the field of a strong laser wave, *Eur. Phys. J. C* **36**, 127 (2004).
- [48] D. V. Karlovets, Radiative polarization of electrons in a strong laser wave, *Phys. Rev. A* **84**, 062116 (2011).
- [49] Y.-F. Li, R. Shaisultanov, Y.-Y. Chen, F. Wan, K. Z. Hatsagortsyan, C. H. Keitel, and J.-X. Li, Polarized Ultrashort Brilliant multi-GeV  $\gamma$  Rays Via Single-Shot Laser-Electron Interaction, *Phys. Rev. Lett.* **124**, 014801 (2020).
- [50] H. Ohgaki, T. Noguchi, S. Sugiyama, T. Yamazaki, T. Mikado, M. Chiwaki, K. Yamada, R. Suzuki, and N. Sei, Linearly polarized photons from compton backscattering of laser light for nuclear resonance fluorescence experiments, *Nucl. Instrum. Methods Phys. Res., Sect. A* **353**, 384 (1994).
- [51] I. F. Ginzburg, G. L. Kotkin, S. L. Panfil, V. G. Serbo, and V. I. Telnov, Colliding  $\gamma e$  and  $\gamma\gamma$  beams based on single-pass  $e^+e^-$  accelerators II. Polarization effects, monochromatization improvement, *Nucl. Instrum. Methods Phys. Res.* **219**, 5 (1984).
- [52] L. Dongguo, K. Yokoya, T. Hirose, and R. Hamatsu, Transition probability and polarization of final photons in nonlinear Compton scattering for linearly polarized laser, *Jpn. J. Appl. Phys.* **42**, 5376 (2003).
- [53] S. Tang, B. King, and H. Hu, Highly polarised gamma photons from electron-laser collisions, [arXiv:2003.03246](https://arxiv.org/abs/2003.03246).

- [54] B. King and S. Tang, Nonlinear Compton scattering of polarised photons in plane-wave backgrounds, *Phys. Rev. A* **102**, 022809 (2020).
- [55] B. King and N. Elkina, Vacuum birefringence in high-energy laser-electron collisions, *Phys. Rev. A* **94**, 062102 (2016).
- [56] Y. Nakamiya and K. Homma, Probing vacuum birefringence under a high-intensity laser field with  $\gamma$ -ray polarimetry at the GeV scale, *Phys. Rev. D* **96**, 053002 (2017).
- [57] S. Bragin, S. Meuren, C. H. Keitel, and A. Di Piazza, High-Energy Vacuum Birefringence and Dichroism in an Ultrastrong Laser Field, *Phys. Rev. Lett.* **119**, 250403 (2017).
- [58] D. Y. Ivanov, G. L. Kotkin, and V. G. Serbo, Complete description of polarization effects in  $e^+e^-$  pair production by a photon in the field of a strong laser wave, *Eur. Phys. J. C* **40**, 27 (2005).
- [59] K. Krajewska and J. Z. Kamiński, Breit-Wheeler process in intense short laser pulses, *Phys. Rev. A* **86**, 052104 (2012).
- [60] B. King, N. Elkina, and H. Ruhl, Photon polarization in electron-seeded pair-creation cascades, *Phys. Rev. A* **87**, 042117 (2013).
- [61] A. A. Sokolov and I. M. Ternov, *Synchrotron Radiation* (Akademik, Berlin, 1968).
- [62] V. N. Baier, V. M. Katkov, and V. S. Fadin, *Radiation from Relativistic Electrons* (Atomizdat, Moscow, 1973).
- [63] K. Kirsebom, Y. V. Kononets, U. Mikkelsen, S. P. Møller, E. Uggerhøj, T. Worm, K. Elsener, C. Biino, S. Ballestrero, P. Sona, R. O. Avakian, K. A. Ispirian, S. P. Taroian, S. H. Connell, J. P. F. Sellschop, and Z. Z. Vilakazi, Generation and detection of the polarization of multi-GeV photons by use of two diamond crystals, *Phys. Lett. B* **459**, 347 (1999).
- [64] U. I. Uggerhøj, The interaction of relativistic particles with strong crystalline fields, *Rev. Mod. Phys.* **77**, 1131 (2005).
- [65] A. Apyan, R. O. Avakian, B. Badelek, S. Ballestrero, C. Biino, I. Birol, P. Cenci, S. H. Connell, S. Eichblatt, T. Fonseca, A. Freund, B. Gorini, R. Groess, K. Ispirian, T. J. Ketel, Y. V. Kononets, A. Lopez, A. Mangiarotti, B. van Rens, J. P. F. Sellschop, M. Shieh, P. Sona, V. Strakhovenko, E. Uggerhøj, U. I. Uggerhøj, G. Unel, M. Velasco, Z. Z. Vilakazi, and O. Wessely (NA59 Collaboration), Coherent bremsstrahlung, coherent pair production, birefringence, and polarimetry in the 20–170 GeV energy range using aligned crystals, *Phys. Rev. ST Accel. Beams* **11**, 041001 (2008).
- [66] K. Yokoya, *CAIN2.42 Users Manual* [<https://ilc.kek.jp/~yokoya/CAIN/Cain242/>].
- [67] F. Lei, A. J. Dean, and G. L. Hills, Compton polarimetry in  $\gamma$ -ray astronomy, *Space Sci. Rev.* **82**, 309 (1997).
- [68] M. L. McConnell and P. F. Bloser, Status and future prospects for  $\gamma$ -ray polarimetry, *Chin. J. Astron. Astrophys.* **6**, 237 (2006).
- [69] M. Eingorn, L. Fernando, B. Vlahovic, C. Ilie, B. Wojtsekhowski, G. M. Urciuoli, F. De Persio, F. Meddi, and V. Nelyubin, High-energy photon polarimeter for astrophysics, *J. Astron. Telesc. Instrum. Syst.* **4**, 011006 (2018).
- [70] C. Ilie,  $\gamma$ -ray polarimetry: A new window for the nonthermal universe, *Publ. Astron. Soc. Pacif.* **131**, 111001 (2019).
- [71] B. Wojtsekhowski, D. Tedeschi, and B. Vlahovic, A pair polarimeter for linearly polarized high-energy photons, *Nucl. Instrum. Methods Phys. Res., Sec. A* **515**, 605 (2003).
- [72] P. Gros, S. Amano, D. Attié, P. Baron, D. Baudin, D. Bernard, P. Bruel, D. Calvet, P. Colas, S. Daté, A. Delbart, M. Frodin, Y. Geerebaert, B. Giebels, D. Götz, S. Hashimoto, D. Horan, T. Kotaka, M. Louzir, F. Magniette, Y. Minamiyama, S. Miyamoto, H. Ohkuma, P. Poilleux, I. Semeniouk, P. Sizun, A. Takemoto, M. Yamaguchi, R. Yonamine, and S. Wang, Performance measurement of HARPO: A time projection chamber as a  $\gamma$ -ray telescope and polarimeter, *Astropart. Phys.* **97**, 10 (2018).
- [73] J. Koga, T. Z. Esirkepov, and S. V. Bulanov, Nonlinear Thomson scattering in the strong radiation damping regime, *Phys. Plasmas* **12**, 093106 (2005).
- [74] V. N. Baier, V. M. Katkov, and V. M. Strakhovenko, *Electromagnetic Processes at High Energies in Oriented Single Crystals* (World Scientific, Singapore, 1998).
- [75] A. Ilderton, Note on the conjectured breakdown of QED perturbation theory in strong fields, *Phys. Rev. D* **99**, 085002 (2019).
- [76] A. Di Piazza, M. Tamburini, S. Meuren, and C. H. Keitel, Improved local-constant-field approximation for strong-field QED codes, *Phys. Rev. A* **99**, 022125 (2019).
- [77] A. Di Piazza, M. Tamburini, S. Meuren, and C. H. Keitel, Implementing nonlinear Compton scattering beyond the local-constant-field approximation, *Phys. Rev. A* **98**, 012134 (2018).
- [78] C. P. Ridgers, J. G. Kirk, R. Ducloux, T. G. Blackburn, C. S. Brady, K. Bennett, T. D. Arber, and A. R. Bell, Modelling  $\gamma$ -ray photon emission and pair production in high-intensity laser-matter interactions, *J. Comput. Phys.* **260**, 273 (2014).
- [79] N. V. Elkina, A. M. Fedotov, I. Yu. Kostyukov, M. V. Legkov, N. B. Narozhny, E. N. Nerush, and H. Ruhl, QED cascades induced by circularly polarized laser fields, *Phys. Rev. ST Accel. Beams* **14**, 054401 (2011).
- [80] D. G. Green and C. N. Harvey, SIMLA: Simulating particle dynamics in intense laser and other electromagnetic fields via classical and quantum electrodynamics, *Comput. Phys. Commun.* **192**, 313 (2015).
- [81] W. H. McMaster, Matrix representation of polarization, *Rev. Mod. Phys.* **33**, 8 (1961).
- [82] L. H. Thomas, The motion of the spinning electron, *Nature (London)* **117**, 514 (1926).
- [83] L. H. Thomas, The kinematics of an electron with an axis, *Philos. Mag.* **3**, 1 (1927).
- [84] V. Bargmann, L. Michel, and V. L. Telegdi, Precession of the Polarization of Particles Moving in a Homogeneous Electromagnetic Field, *Phys. Rev. Lett.* **2**, 435 (1959).
- [85] See Supplemental Material at <http://link.aps.org/supplemental/10.1103/PhysRevResearch.2.032049> for details on the employed laser fields, the applied theoretical model, and the simulation results for other laser or electron parameters.
- [86] Y. I. Salamin and C. H. Keitel, Electron Acceleration by a Tightly Focused Laser Beam, *Phys. Rev. Lett.* **88**, 095005 (2002).
- [87] A. J. Gonsalves, K. Nakamura, J. Daniels, C. Benedetti, C. Pieronek, T. C. H. de Raadt, S. Steinke, J. H. Bin, S. S. Bulanov, J. van Tilborg, C. G. R. Geddes, C. B. Schroeder, Cs. Tóth, E. Esarey, K. Swanson, L. Fan-Chiang, G. Bagdasarov, N. Bobrova, V. Gasilov, G. Korn, P. Sasorov, and W. P. Leemans, Petawatt Laser Guiding and Electron Beam Acceleration to 8 GeV in a Laser-Heated Capillary Discharge Waveguide, *Phys. Rev. Lett.* **122**, 084801 (2019).
- [88] M. Placidi and R. Rossmannith,  $e^+e^-$  polarimetry at LEP, *Nucl. Instrum. Methods Phys. Res., Sec. A* **274**, 79 (1989).